CSIRO Publishing

Functional Plant Biology

Continuing *Australian Journal of Plant Physiology*

VOLUME 29, 2002

All enquiries and manuscripts should be directed to:

Functional Plant Biology
CSIRO Publishing
PO Box 1139 (150 Oxford St)
Collingwood, Vic. 3066, Australia

Telephone: +61 3 9662 7625
Fax: +61 3 9662 7611
Email: publishing.fpb@csiro.au

Published by CSIRO Publishing
for CSIRO and the Australian Academy of Science

www.publish.csiro.au/journals/fpb

Funct. Plant Biol., 2002, **29**, 1259–1272

Space and time dependence of temperature and freezing in evergreen leaves

Marilyn C. Ball[A,F], *Joe Wolfe*[C], *Martin Canny*[A], *Martin Hofmann*[B], *Adrienne B. Nicotra*[D] *and Dale Hughes*[E]

[A]Ecosystem Dynamics and [B]Visual Sciences, Research School of Biological Sciences, Institute of Advanced Studies, Australian National University, Canberra, ACT 0200, Australia.
[C]School of Physics, University of New South Wales, Sydney, NSW 2052, Australia.
[D]Department of Botany and Zoology, Australian National University, Canberra, ACT 0200, Australia.
[E]CSIRO Division of Land and Water, Canberra, ACT 2601, Australia.
[F]Corresponding author; email: mball@rsbs.anu.edu.au

Abstract. Infrared video thermography was used to study space and time dependence of freezing in intact, attached leaves of snow gum (*Eucalyptus pauciflora* Sieb. ex Spreng.) seedlings. Freezing initiated in the midvein and spread through the apoplast at 10 mm s^{-1}. Freezing of apoplastic water was detected by a local, rapid increase in temperature, and was followed by a slower increase in leaf temperature to the equilibrium freezing temperature as symplastic water moved from cells to extracellular sites of ice formation. The duration of freezing varied with position, leaf thickness and water content. Most of the cellular water in the leaf tip and margins froze quickly, while freezing was slower near the petiole and midvein. Regions that had frozen more rapidly then began to cool more rapidly, producing steep gradients in leaf temperatures and hence also freeze-induced dehydration. Thus, spatial variation in physical properties of leaves could affect the distribution of minimum leaf temperatures, and hence, the distribution and extent of damage due to freeze-induced dehydration. These results are consistent with patterns of freezing damage in autumn when the duration of freezing may be insufficient for the whole leaf to freeze before sunrise, and may explain the general observation of increased leaf water content and thickness with altitude.

Introduction

Much recent progress has been made on the cellular (Steponkus *et al.* 1993; Uemura and Steponkus 1999), molecular (Thomashow 1999; Xin and Browse 2000) and biophysical (Wolfe and Bryant 1999) bases of freezing injury and tolerance in plants. Such studies provide fundamental insight into the effects of freezing on ultrastructural and cellular components of tissues. Much of this work concerns scales of, say, tens of microns or less, where variations in temperature are very small because the thermal conductivity of wet tissue removes substantial temperature gradients. However, at higher levels of organization (a scale of, say, millimetres) there can be much larger differences in temperature, and this raises a new set of questions. Why do such differences occur in a leaf exposed to air of a particular temperature and to a particular radiation background? Why is it that some regions first become cold enough to freeze? How do they nucleate freezing in the neighbours? What happens to the latent heat liberated during freezing? How fast does freezing occur, and is there sufficient time for osmotic equilibration? Answers to such questions are fundamental to understanding spatial patterns in freezing injury of complex tissues such as leaves.

Consider the two leaves shown in Fig. 1. Both leaves are the same age, with differences in appearance reflecting differences in exposure to freezing temperatures. The green leaf is from a seedling grown under protected glasshouse conditions, whereas the necrotic areas and red pigmentation in the other leaf developed after exposure to an early autumn frost. Note the pattern of freezing injury. The necrotic areas are visible along the leaf margins, particularly near the leaf tip. A red pigment, anthocyanin, colours the veins and is distributed differentially over the lamina. The apparent concentration of anthocyanin in the lamina is lowest near the midvein and increases toward leaf margins, with the greatest concentrations occurring near the leaf tip. This pattern is typical of snow gum leaves exposed to mild freezing stress. The same pattern occurs under more severe autumn conditions, when necrotic areas expand from the leaf tip and margins toward the centre and petiole. This pattern invites the question, why is freezing damage to the lamina greatest

Abbreviations used: SEM, scanning electron microscopy; t, time; T, temperature; T_a, T_b, T_e, T_f, T_n, air, background, equilibrium, freezing and nucleation temperature, respectively.

10.1071/FP02037 1445-4408/02/111259

along leaf margins? Here, we explore this question by studying time and space dependence of freezing in intact, attached leaves of field-grown snow gum seedlings.

Theory

The experiments in our study yield $T(x, y, t)$, the dependence of temperature (T) on time (t) and position (x, y) in the plane of the leaf. The prediction and analysis of such data are complicated because the leaf is inhomogeneous in (x, y). Thinner areas with lower heat capacity cool more quickly at the same rate of heat loss. Further, some parts lose heat more rapidly than others because of their location. The edges and particularly the tip of the leaf radiate heat into a larger solid angle than do other regions, and they also lose heat by conduction more readily because of a thinner boundary layer. Finally, some regions of the leaf freeze more easily. For simplicity, however, the sketch in Fig. 2 shows key features of $T(t)$ for a small, thermally-homogeneous section of a leaf with fixed water content. We discuss its behaviour qualitatively here, and give mathematical details in the appendix. At any pair of temperatures, T_b of the background and T_a of the air, there is a temperature (T_e) at which a leaf would be in thermal equilibrium with both. At this temperature the rate of heat absorption by the leaf (radiation and conduction) exactly balances that of heat lost by these mechanisms. If leaf temperature (T) is greater than T_e, then the leaf loses heat. In the experiments reported here, $T_b(t)$ and $T_a(t)$ are very similar functions of time. Subject to this condition, a curve of $T_e(t)$ is slightly displaced from a curve of $T_b(t)$ or $T_a(t)$, but its displacement is nearly constant with time unless freezing causes a major change in the emissivity, reflectance or local geometry of the leaf. In the model, then, $T_e(t)$ follows $T_b(t)$ or $T_a(t)$ closely and is qualitatively very similar to them, even when leaf temperature does not follow $T_b(t)$ or $T_a(t)$.

In the model $T(t)$ sketch (Fig. 2), as in our experiments, a leaf near room temperature is inserted into a pre-chilled chamber where air and background temperatures decline at a constant rate. Initially because $T > T_e$, the leaf loses heat relatively rapidly, and $T(t)$ falls more rapidly than does T_e. Because the section is assumed to be homogeneous, and because T_e decreases linearly with time, $T(t)$ approaches $T_e(t)$ approximately exponentially. Leaf temperature then declines linearly in response to decreasing environmental temperature until nucleation of ice in extracellular water occurs at T_n. Then, liberation of latent heat as water condenses from liquid or vapour to a crystalline state causes leaf temperature

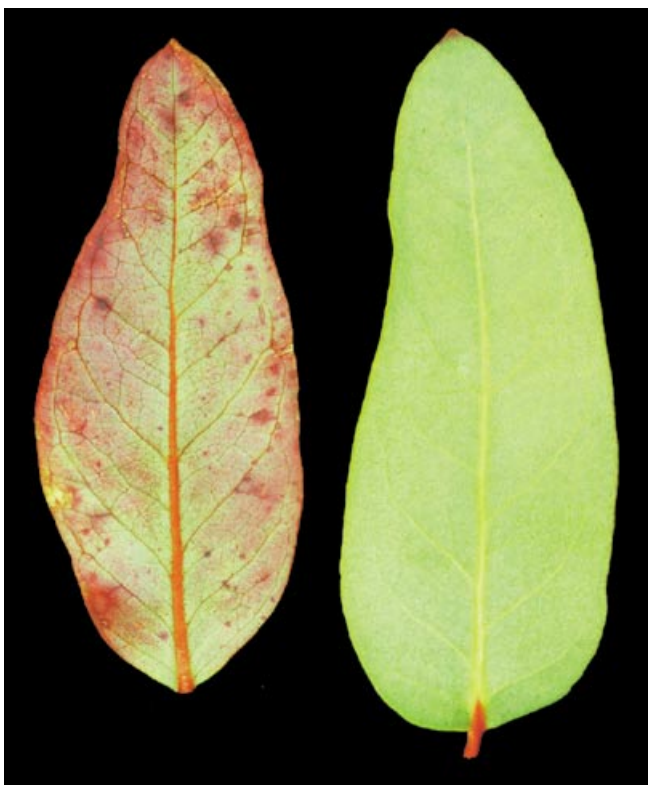

Fig. 1. Colour photograph of leaves of snow gum (*Eucalyptus pauciflora*) seedlings that were either protected from freezing temperatures under glasshouse conditions (right) or subject to natural early autumn frost under field conditions (left).

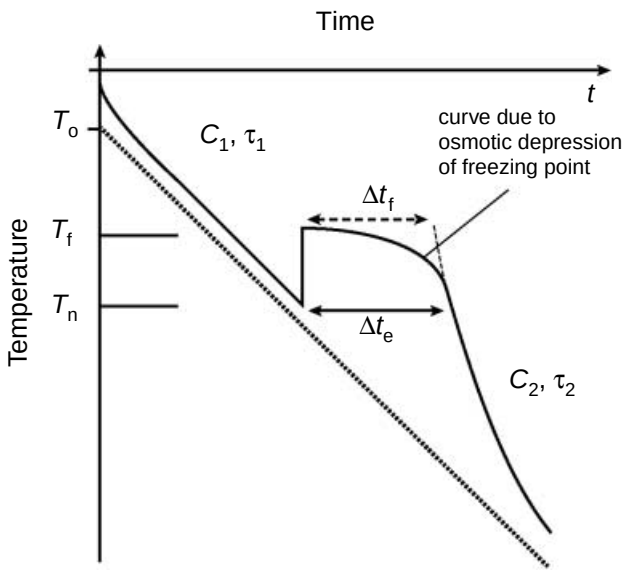

Fig. 2. Sketch showing expected thermal behaviour of a homogeneous leaf sample with fixed water content subject to a constant rate of environmental cooling. A detailed explanation is given in the 'Theory' section of the text. T_o, leaf temperature at time zero; T_n, ice nucleation temperature; T_f, equilibrium freezing temperature; Δt_e, duration of time when leaf temperature was elevated above nucleation temperature during freezing; C_1, C_2, heat capacity of leaf before freezing and after most leaf water has frozen, respectively; τ_1, τ_2, characteristic times for cooling before freezing and after most leaf water has frozen, respectively. Dotted and solid lines indicate environmental and leaf temperatures, respectively. Dashed line shows a hypothetical isothermal phase of duration Δt_f that would occur if there were no osmotic effects on T_f.

to rise to the equilibrium freezing temperature, T_f. When an amount of supercooled water freezes, the liberation of latent heat would be sufficient to raise its own temperature by $L/c_w = 80$ K, where L is the latent heat of freezing and c_w the specific heat of water. This does not happen because freezing only continues while the temperature remains below or at T_f. Thus, the latent heat diffuses quickly to surrounding tissue, warming it to T_f. The mass of tissue thus warmed may exceed the mass of the tissue freezing by a ratio of order $80\text{K}/(T_f - T_n)$. As freezing continues at T_f, heat loss initially results not in a change in temperature, but in a change in the fraction of the region that is frozen. Thus, the sketch of $T(t)$ shows an abrupt rise from T_n to T_f, and then a region that is initially nearly horizontal. If there were no osmotic effects temperature would remain at or close to T_f until all available water was frozen, as indicated by the isothermal phase of duration Δt_f in Fig. 2. If no water were transported into the freezing region from elsewhere, then freezing would cease after a few minutes (Δt_f) and that icy tissue would then cool rapidly, with the slope of $T(t)$ gradually becoming less negative as the tissue temperature approached $T_e(t)$.

Osmotic effects complicate the freezing process. Ice has a lower vapour pressure and chemical potential than pure liquid water at the same subzero temperature. Once the temperature of extracellular ice is even marginally below the T_f of an intracellular solution, water flows or diffuses from the cell to sites of ice formation, thereby dehydrating the cell. As the concentration of solutes in the remaining cellular water rises, T_f falls due to osmotic freezing-point depression, thereby keeping the chemical potential of the cooling ice and the unfrozen cellular water approximately equal, at least on time-scales longer than a few tens of seconds, the time for hydraulic equilibration of a typical cell (Wolfe and Bryant 1992). The amount of water that must be lost from a cell before equilibrium is reached between intracellular water and extracellular ice depends on the temperature and osmotic properties of the cell. The water potential of ice declines by approximately 1.2 MPa $°C^{-1}$, requiring an equivalent increase in solute concentration in cellular water of approximately 500 osmol m^{-3} $°C^{-1}$. The increase in solute concentration with dehydration is approximately inversely proportional to cell volume. It follows that large changes in cell volume (several tens of percent) are required to maintain equilibrium for a 1°C drop in temperature near the freezing point compared with lower temperatures. [For instance, for a cell with an initial osmotic pressure of 0.8 MPa, the equilibrium freezing temperature is about –1°C. Cooling to –2°C requires the solute concentration in the (unfrozen) cytoplasm to increase by a factor of approximately 2 (1.6 MPa), and so an aqueous volume reduction of roughly 2 (V_0 to $V_0/2$). Further cooling to –3°C requires an approximately equal increase in osmotic pressure (~1.6 to ~2.4 MPa), so the concentration must be increased by a factor of about 3/2, which requires the aqueous volume to be reduced by a factor of about 2/3 (~$V_0/2$ to $V_0/3$).] Thus, as more water freezes, the freezing temperature falls in the way shown in Fig. 2. As the remaining unfrozen solution becomes smaller while the number of dissolved solutes remains constant, the rate of decrease in the freezing temperature becomes successively greater, leading to the convex-up part of the curve.

After a while, the rate of freezing falls. The remaining water either has a very high solute concentration and therefore is difficult to freeze, or is isolated from nucleation by physical barriers or colloidal effects (Wolfe and Bryant 1999). The leaf is still rather warmer than T_e, so once again it begins to cool rapidly. The cells continue to dehydrate as the leaf cools, but the rate of freezing becomes too slow for the heat released to sustain an elevation in leaf temperature. If the rate of further freezing were very small, and if no water is brought into the freezing region, this would give rise to a Newtonian cooling phase in which $T(t)$ is concave-up, as shown in Fig. 2. Finally, $T(t)$ would approach $T_e(t)$, i.e. it becomes approximately linear with time. Importation of water would prolong freezing and slow cooling.

The description given above is complicated by inhomogeneities. Firstly, the parameters vary with position, which produces inhomogeneities in T. Secondly, these inhomogeneities in T produce heat conduction in the plane of the leaf. Thirdly, osmotic inhomogeneities give rise to water redistributions during freezing. We return to these complications in the 'Discussion' section.

Materials and methods

Plant material and cultivation

Seeds of *Eucalyptus pauciflora* Sieb. ex Spreng. were collected from three trees growing on the floor of the Orroral Valley at an elevation of 850 m in New South Wales, Australia. Seeds were cold stratified under moist conditions at 3°C for 4 weeks before germination on sand flats in a mist house. Similar seedlings of average size were transferred to individual containers filled with soil and grown either under glasshouse conditions in Canberra, or in a pasture subject to frequent frosts (elevation 700 m) at Bungendore, New South Wales (Ball *et al.* 1997). Pots were 400 mm deep and made of 155 mm internal diameter PVC storm-water pipe fitted with a shade-cloth cover on the bottom. Seedlings were 1-year old at the time of study.

Imaging leaf water contents

Five leaves of field-grown snow gum seedlings (one leaf per seedling) were cut under water and transported to the laboratory in a styrofoam container filled with damp paper towels. Leaves were blotted dry, then placed on a computer-controlled constant motion platform that conveyed the leaves past a CASI spectrographic imaging system (Itres, Calgary, Canada). Illumination (photosynthetic photon flux density of 400 μmol m^{-2} s^{-1}) was provided with halogen lamps. Reflected radiation was recorded in 3.6-nm steps from 750 to 928 nm for each pixel, with a spatial resolution of 0.22 mm per pixel. Reflectance was calculated by dividing the radiation reflected from leaves by radiation reflected from a calibrated white standard coated with barium sulfate. After scanning, five discs (8 mm diameter) were punched from each leaf and placed into individual pre-weighed eppendorf vials. The

punches were arranged at five evenly-spaced positions along the length of the lamina to capture changes in amounts of water and dry matter per unit leaf area from leaf tip to petiole. These relative positions allowed comparison of similar regions of leaves differing in length. Each leaf was then re-scanned so that the positions of punches could be mapped onto the original leaf scans to obtain the reflectance characteristics of each disc before cutting. Vials were weighed to determine fresh weight of discs. Discs were then transferred to individual paper envelopes for oven drying at 80°C for 24 h before determining dry weight of each disc. All measurements were made with a high precision balance (AT21 Comparator; Mettler-Toledo, Greifensee, Switzerland). A reflective index of water content per unit leaf area was calculated according to Peñuelas *et al.* (1997) based on the difference between the average reflectance measured at a reference waveband (R_r; here 850 nm) and that measured in a region affected by the absorbance of near infrared radiation by water (R_w; here the average from 914 to 928 nm).

Cryo-scanning electron microscopy

Leaves on five snow gum seedlings that had been grown for a year in a glasshouse were selected for study. Three leaves were selected on each plant and allocated to one of three treatments: control, or frozen at either –2 or –5°C. Leaves remained intact and attached until samples were collected for analysis by cryo-scanning electron microscopy (cryo-SEM). Control leaves were left at room temperature, while freezing treatments were imposed on leaves covered with a thin plastic sheath and gently submerged in a computer-controlled bath at 5°C. The bath temperature was then decreased for 30 min to –2°C. A small amount of ice was sprinkled over the leaves in each bag to promote freezing, and leaves were incubated at –2°C for a further 30 min. Then, samples of leaves allocated to the –2°C treatment were collected by snap-freezing with cryo-pliers cooled to –196°C before the bath temperature was lowered at 2°C h^{-1} to –5°C. Cryo-pliers were again used to snap-freeze samples from leaves allocated to the –5°C treatment after incubation at –5°C for 30 min. Frozen samples were held in cryo-storage at liquid nitrogen temperature until examined in the cryo-SEM.

For observation, frozen leaf samples were trimmed under liquid nitrogen to 4 × 4 mm squares and mounted with Tissue Tek (Sakura Finetechnical Co., Tokyo, Japan) in slots in aluminium stubs. These stubs were transferred under liquid nitrogen to the stage of a cryo-microtome (CR 2000; Research and Manufacturing Inc., Tucson, AZ, USA) where the leaf was planed with glass and diamond knives to give a smooth transverse face. The stub was then transferred under liquid nitrogen to the cryo-preparation chamber (CT 5000; Oxford Instruments, Eynsharm, UK), and hence to the cold stage of the cryo-SEM (JSM 6400; JEOL Ltd, Tokyo, Japan) where it was observed at 1 kV. The surface of the specimen was lightly etched for a minute or so at –90°C to reveal cell outlines, re-cooled, and returned to the cryo-preparation chamber at –160°C. Here it was coated with 50 nm of evaporated aluminium. The specimen was returned to the cryo-stage at –160°C and observed at 15 kV. Micrographs were recorded on Kodak Tmax 120 roll-film developed in Tmax developer. Further details of this technique are given in Huang *et al.* (1994).

Freezing kinetics

Infrared video thermography (Wisniewski *et al.* 1997) was used to determine the kinetics of freezing in intact attached leaves of seedling snow gum, *E. pauciflora*. Measurements were made with an Aegema 870 infrared video camera (Danderyd, Sweden) fitted in a leaf-cooling chamber as described in Lutze *et al.* (1998). Air temperature at leaf height in the freezing chamber was monitored with a platinum resistance thermometer and regulated by a computer-controlled water bath that enabled slow, steady rates of cooling (Julabo, Seelbach, Germany).

Freeze tolerance

Electrolyte leakage from leaf cells was determined according to Webb *et al.* (1996) with a few modifications. Measurements were made on five fully-expanded leaves of similar age, one leaf from each of five plants. Eight discs (8 mm diameter) were cut from the lamina of each leaf and randomly assigned to eight temperature treatments, giving five replicates (i.e. one disc from each leaf) for each treatment. Discs were placed in individual test tubes cooled to 5°C in a computer-controlled refrigerated water bath (Julabo). The temperature was lowered to –2°C for 30 min, before nucleation was initiated by addition of a small amount of ice. Discs were incubated at –2°C for 60 min before measurements began. Temperature was then decreased in 1°C steps, allowing 5 min to reach each new temperature, followed by incubation at the designated temperature for 30 min. Five leaf discs were removed after 30 min at each nadir temperature and thawed in the dark for 10 min at room temperature before addition of deionized water. Intactness of leaf cells was assayed as the percentage change in conductivity following dark incubation of discs in deionized water at 3°C for 24 h, before and after breakage of cells by immersion of leaf discs in liquid nitrogen (Webb *et al.* 1996).

Statistics

GenStat 5, version 4.1 (Numerical Algorithms Group, Oxford, UK) was used to analyse data by ANOVA.

Results

Spatial variation in leaf properties

Fully-expanded leaves of snow gum seedlings showed spatial variation in properties that could affect freezing of leaf tissue. For example, average thickness of the leaf lamina increased 50% from 0.44 mm near the leaf tip to 0.66 mm near the petiole (Table 1). This increase in thickness was accompanied by a 21% average increase in fresh weight per unit area, due to greater amounts of both dry matter and water per unit area near the petiole. However, the relative proportions of dry matter and water varied with thickness, with fractional water content increasing an average of 2% from the leaf tip to the petiole. This corresponded to a 25%

Table 1. Variation in lamina properties along sagittal transects from leaf tip to petiole

Values are means (n = 5 leaves) of discs collected at relative positions along the leaf lamina. LSD, least significant difference between means as determined by ANOVA. All parameters increased significantly (P<0.03) with distance from leaf tips. Heat capacity per leaf area was calculated using the specific heat capacity of liquid water at 20°C (i.e. 4182 J kg^{-1} K^{-1}), and assuming the value for dry matter to be one-third that for water

Parameter	LSD	Position (from leaf tip to petiole) 1	2	3	4	5
Thickness (mm)	0.04	0.44	0.46	0.50	0.54	0.66
Fresh weight (g m^{-2})	28	486	488	506	522	588
Fractional water content	0.018	0.653	0.655	0.658	0.665	0.673
Water per unit area (g m^{-2} at 20°C)	23	310	313	325	339	389
Heat capacity per area (kJ m^{-2} K^{-1})	0.07	1.54	1.55	1.61	1.67	1.97

average increase in water content per unit leaf area from 310 g m^{-2} in the thinnest regions of the lamina to 389 g m^{-2} in the thickest regions near the petiole.

Water distribution within leaves was assayed by spatial variation in reflectance due to absorbance of near infrared radiation by water. The absorption spectrum of water shows four major peaks, with the water content of leaves being best correlated with differences in reflectance due to absorption at 970 nm (Peñuelas *et al.* 1997). In well-hydrated leaves, this is manifest in a trough in reflectance, with minimal values occurring between 950 and 970 nm (Peñuelas *et al.* 1997). We were not able to measure at wavelengths greater than 928 nm, but found that measurements made on the shoulder of the reflectance trough were correlated significantly ($P<0.01$) with leaf water content (Fig. 3*A*). The relationship was noisy, but no more so than measurements made between 950 and 970 nm (Peñuelas *et al.* 1997), and was used to create a map of the spatial distribution of water in one young, fully-expanded leaf (Fig. 3*B*). This map shows marked spatial variation in water contents dependent on both tissue type and position within the leaf. Water contents per unit leaf area were greatest in the midvein near the petiole. In this region, for example, a transect across the leaf (Fig. 3*B*) shows more water in veins than in adjacent lamina, with water contents declining from 670 g m^{-2} in the midvein to 350 g m^{-2} in a vein closer to the leaf margin. The amount of water associated with both veins and lamina, and the differences in water content between them, declined with distance from the petiole toward the leaf tip (Fig. 3*B*).

Freezing of intact attached leaves

The distribution of ice and associated anatomical changes within freezing leaves were explored via cryo-SEM to gain insight into the nature of freeze-induced damage to the leaf lamina. Cryo-SEM images of intact attached leaves at temperatures from +20 to –5°C are shown in Figs 4*A–F*. There was a striking contrast between control leaves and those slowly frozen to –5°C (Figs 4*A*, *B*). Control leaves at 20°C (Fig. 4*A*) showed normal anatomical features. The internal appearance of the leaves with a double layer of palisade is typical of eucalypt leaves with isobilateral symmetry. The cryo-preparation procedure did not alter cell volumes significantly, nor form any ice crystals on exterior surfaces of cell walls (Fig. 4*C*). The cell vacuoles revealed by planing through cells showed lacy, eutectic lines typical of solute-rich spaces prepared by this technique (Fig. 4*C*).

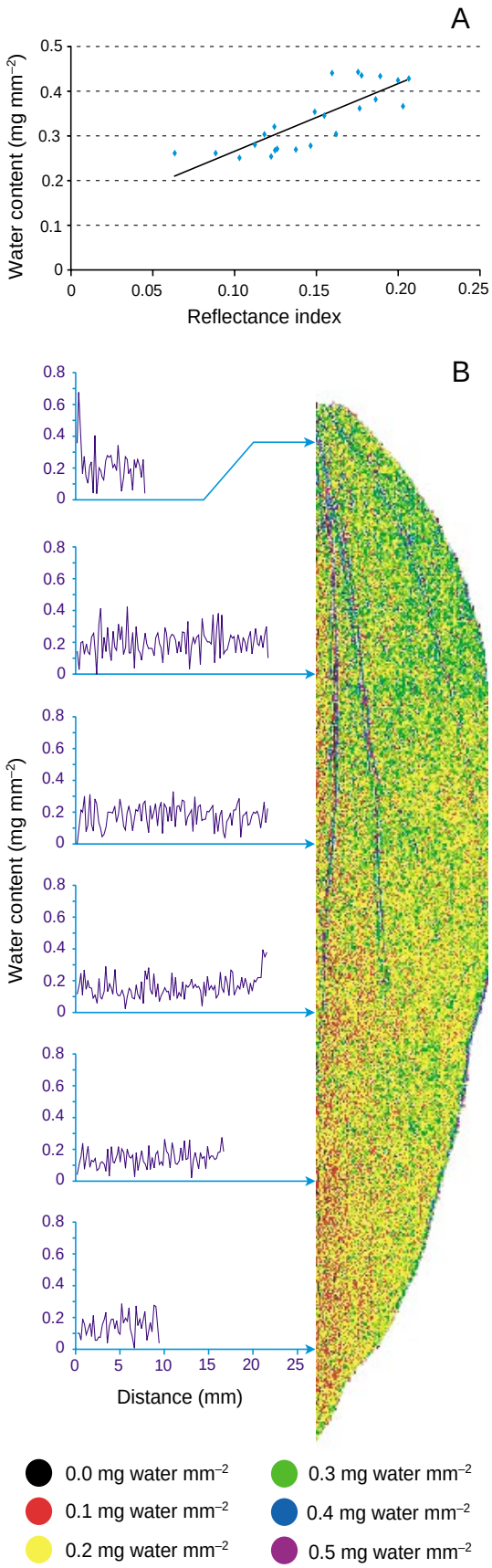

Fig. 3. Spatial variation in water content in leaves of snow gum (*Eucalyptus pauciflora*) seedlings. (*A*) Average reflectance index as a function of leaf water content. The line drawn by linear regression fits the equation $y = 0.113 + 1.512x$ ($r^2=0.67$, $P<0.0001$). (*B*) Spatial distribution of water in a snow gum leaf. The map was drawn by applying the average relationship shown in Fig. 3*A* to reflectance data from one leaf. Pixel width is 0.2 mm.

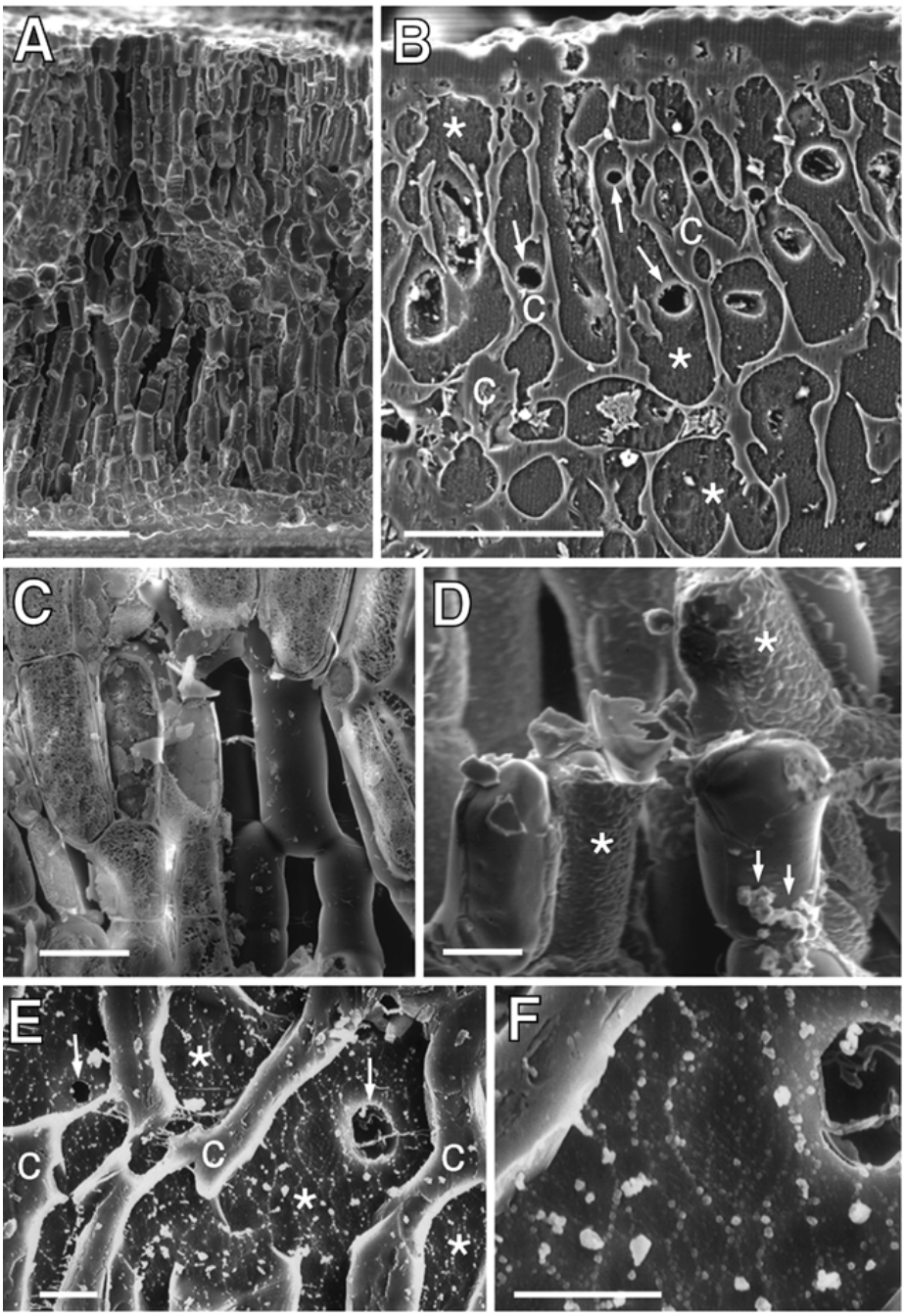

Fig. 4. Cryo-SEM images of frozen, fully-hydrated leaf specimens of snow gum (*Eucalyptus pauciflora*) stabilized by snap-freezing before and during experimental slow freezing. All images are transverse faces of planed leaf laminas. (*A*) Complete thickness of a control leaf at 20°C. Scale bar, 100 μm. (*B*) Epidermis and adjacent palisade tissue of a leaf slowly cooled to –5°C. Extracellular ice (∗) surrounds shrunken cells (c) and entraps air bubbles (arrows) that are relics of intercellular air spaces. Scale bar, 100 μm. (*C*) Mesophyll cells in a control leaf at 20°C. Most cells were cut open by the planing, revealing sections through cell walls and solute-rich vacuoles filled with lacy eutectic domains. Surfaces of three intact cells are seen at right of centre. Scale bar, 20 μm. (*D*) Developing layer of extracellular ice (∗) on mesophyll cell walls in a leaf slowly cooled to –2°C. Note ice crystals (arrows) in foreground. Scale bar, 10 μm. (*E*) Extensive development of extracellular ice in the lamina of a slowly-cooled leaf after 30 min at –2°C. Symbols as in *B*. Note pectic strands (arrowheads) linking cells to each other. Scale bar, 10 μm. (*F*) Close-up view from *E* showing a shrunken cell, extracellular ice, and remains of an intercellular air space. Note globular eutectic domains arrayed within the ice. Scale bar, 10 μm.

Thus, although the rate of cryo-freezing was not fast enough for vitrification, there was no evidence of water movement out of cells during preparation. These patterns are consistent with those reported in exhaustive studies of the reliability of the technique (Huang *et al.* 1994; McCully *et al.* 2000).

The slow experimental freeze at –2°C in the presence of external ice induced extracellular freezing in intact attached leaves of snow gum seedlings. In images from the early stages of cooling, ice crystals were seen on outer cell wall surfaces and enveloped cell walls (Fig. 4*D*). The extracellular ice mass grew at the expense of cell volume as water moved from cells to sites of ice formation (Fig. 4*E*), leaving the intact cell walls shrunken and distorted (Fig. 4*E*). There was no evidence of wall rupture or plasmolysis — cell walls appeared to remain in contact with their dehydrating cells (Fig. 4*E*). Ice filled the spaces between cells, entrapping air bubbles, which were the residue of much larger intercellular air spaces like those visible in Fig. 4*A*. Dehydration of mesophyll cells was more extreme in leaves that had been cooled to –5°C (Fig. 4*B*). These shrunken cells were rarely opened by the planing knife, and the nature of their contents is obscure. However, there was no evidence of intracellular ice formation.

Kinetics of freezing in intact attached leaves

We refer to plots of $T(t)$ during cooling as exotherms, because of the similarities to plots of $T(t)$ used in calorimetry. Freezing exotherms were determined in intact attached leaves by infrared thermography of change in leaf surface temperature as the leaf chamber was cooled at a rate of 2°C h^{-1} from 2 to –8°C. Spatial variation, $T(x, y)$, in leaf surface temperatures at selected times during cooling is shown for one leaf in Fig. 5, with corresponding exotherms [$T(t)$] for pixels at three locations along the midvein shown in Fig. 6. Leaf temperatures declined evenly in the cooling chamber, with temperature variation over the leaf surface being less than 0.5°C until freezing began. In all leaves, freezing started in the midvein near the petiole and spread throughout the leaf within 10 s. In the five leaves, nucleation occurred at an average T_n of –3.1 ± 0.4°C, and leaf temperatures subsequently increased to an average T_f of –0.4 ± 0.1°C. Thus, nucleation occurred with approximately 2.7 ± 0.3°C of supercooling.

Many exotherms (e.g. Figs 6*A*, *C*) appeared to show an intermediate peak during increase in leaf temperature from T_n to T_f. A second set of measurements was made with a faster rate of data collection to resolve these changes in leaf temperature during early events in freezing. Spatial variation in leaf surface temperatures at selected times during freezing is shown for one leaf in Fig. 7, with corresponding exotherms for two centrally-located pixels in the midvein and adjacent lamina shown in Fig. 8. In all leaves, freezing began in the thickest region of the midvein near the petiole and propagated rapidly through the leaf at rates of approximately 10 mm s^{-1} (Fig. 7). The first, rapid increase in temperature presumably indicated freezing of vapour plus apoplastic water, with the subsequent slower increase in temperature to T_f apparently occurring as symplastic water moved from cells to extracellular sites of ice formation, consistent with recent studies of freezing in leaves of barley (Pearce and Fuller 2001). The first peak was highly variable and better resolved in the midvein than in the lamina, consistent with greater amounts of apoplastic water in the former (Fig. 8). However, within 5 min after nucleation, T_f was attained throughout the leaf and spatial variation in leaf temperature was less than 0.5°C (Fig. 7).

The duration of elevated temperatures during freezing varied with position in the leaf, increasing from the leaf tip toward the petiole, consistent with increase in thickness and water content (Fig. 6). A useful empirical measure is the time to return to nucleation temperature following the onset of freezing (Δt_e in Fig. 2). Values of Δt_e varied significantly ($P<0.01$) with tissue type and position in a leaf (Fig. 9*A*). Averaged overall, Δt_e was greater in the midvein region than in corresponding areas in the lamina. Values were minimal near the tip, in the thinnest region of the leaves, and increased toward the thickest regions near the leaf petiole.

Leaf temperatures declined rapidly once most of the water in a leaf had frozen (Fig. 6). If water content was constant, then these rates of cooling would depend on the heat capacity of the tissue, rates of energy transfer within the leaf and to its environment, and freezing of the remaining unfrozen water. Note that the trajectories of $T(t)$ during this cooling phase at different positions along the midvein of an exemplary leaf (Fig. 6) differed substantially from the idealized curve shown in Fig. 2. The decline in leaf temperature with time was not simply an exponential approach to the linear asymptote. Indeed, it lacked the distinctive concave-up shape that would be expected with Newtonian cooling. It appears that freezing of the remaining unfrozen solution, or of water imported from elsewhere, released sufficient heat to substantially slow the rates of cooling. Nevertheless, we used an empirical fit having the form of an exponential decay plus a linear fall, and used the characteristic time, τ_2, of the exponential as a purely empirical measure for comparison of spatial variation in cooling. Values of τ_2 varied significantly ($P<0.01$) with tissue type and position in a leaf (Fig. 9*B*). Averaged overall, τ_2 was greater in the midvein region than in corresponding areas in the lamina. Values of τ_2 increased progressively from the leaf tip toward the petiole, with regions near the tip cooling 2.5 times more rapidly than those near the petiole. Thus, regions of the leaf where most of the water froze quickly also cooled more rapidly than those where freezing was more prolonged (Fig. 9). These differences gave rise to the large spatial and temporal gradients in leaf temperature shown in Fig. 5.

Freezing tolerance

This study explores the pattern of freezing damage sustained in early autumn when leaves may not be fully acclimated to freezing temperatures. Thus, it is important to ascertain how the small scale variation in temperatures revealed by the kinetic studies might relate to the distribution of freezing injury in unacclimated leaves. Unacclimated leaf tissue was sensitive to freezing, as indicated by rapid increase in electrolyte leakage with decrease in nadir temperature below –3°C (Fig. 10). Leaf discs incubated at –4°C lost approximately 60% of electrolytes, with maximal electrolyte loss occurring at –6°C. Because of this sensitivity to small changes in temperature, small-scale variation in thermal history could produce major differences in spatial distribution of freezing damage over a leaf surface.

Discussion

It has long been known that the geometry and orientation of leaves in relation to the surrounding environment, particularly sky exposure, have major effects on minimum leaf temperatures, and hence, incidence of freezing temperatures (Leuning 1988; Jordan and Smith 1995; Blennow *et al.* 1998). Whether or not such freezing temperatures lead to frost damage in the foliage depends on many factors. These include the way in which physical properties of leaves influence space and time dependence of extracellular freezing in relation to cellular tolerance of freeze-induced dehydration.

One physical property of leaves that affects time-dependent change in $T(x, y)$ is water content, upon which heat capacity depends. Average water contents ranged from 65–67% of fresh weight per unit area in thin and thick

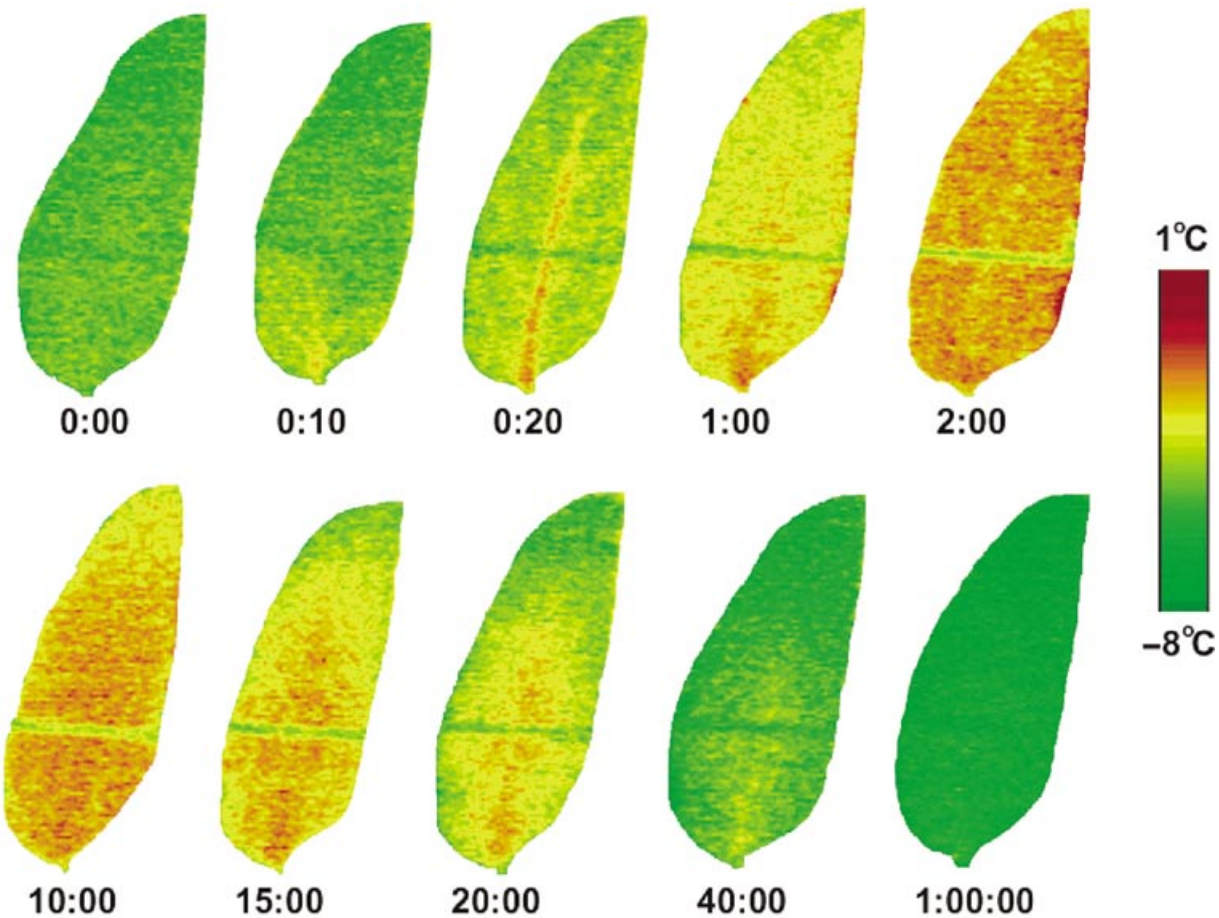

Fig. 5. Spatial variation in leaf surface temperature during freezing of an intact attached leaf of a snow gum (*Eucalyptus pauciflora*) seedling subject to an environmental cooling rate of 2°C h^{-1}. Images are arranged in two groups to illustrate spatial changes in leaf temperature associated with two phases in the freezing process. The first phase is characterized by increase in temperature from T_n to T_f. At time zero, leaf temperatures were similar over the whole leaf surface. Ten seconds later, increase in leaf temperature showed that nucleation had occurred near the petiole. Freezing was widespread throughout the leaf after 20 s, and temperatures continued to increase until T_f was attained. The second phase is characterized by cooling. Temperatures decreased most rapidly near the leaf tip and margins. Temperatures near T_f persisted longest around the midvein toward the petiole, where temperatures remained higher than in other regions of the leaf for at least 40 min after the onset of freezing. Detailed exotherms for three individual pixels from the same leaf are shown in Fig. 6. The line across leaf surfaces is due to a rod holding thermocouples in the air space between the leaf and camera.

regions of the lamina, respectively (Table 1). These values are typical for leaves of sclerophyllous eucalypts (Landsberg 1990; Roderick *et al.* 1999). However, such average values mask small scale inhomogeneities in water content, due to the positions of veins of all sizes and the variation in thickness of leaf tissue (Fig. 3), which are important to ice nucleation, duration of freezing, rates of cooling, and hence also freezing damage.

In the present study, freezing of intact attached leaves always initiated in the midvein near the petiole (Figs 5, 7). This observation is consistent with those of a previous study on detached leaves of snow gum seedlings (Lutze *et al.* 1998). The cause of nucleation is not clear, but it seems unlikely to be due to such extrinsic factors as ice-nucleating bacteria (Lindow *et al.* 1982) or growth of ice crystals through stomata (Wisniewski and Fuller 1999). These factors would induce an apparently random spatial pattern in nucleation over a leaf surface, whereas freezing consistently began where the greatest amount of apoplastic water occurred. It appears that nucleation in the present study occurred in large xylem vessels, as argued by Sakai and Larcher (1987). These results raise questions about roles of hydraulic architecture and vessel wall properties in supercooling and freezing of leaves.

One might expect apoplastic water to freeze before cytoplasmic or vacuolar water because apoplastic water has a higher equilibrium freezing temperature and so is supercooled earlier than cytoplasmic or vacuolar water. Further, the tonoplast and plasma membranes, respectively, compartmentalize vacuolar and cytoplasmic water within cells, whereas xylem vessels contain large, macroscopically contiguous volumes of water. Formation of an ice embryo and attainment of critical size for crystal growth are probabilistic, so the chance of nucleation depends on the volume of available water as well as the concentration of nucleators and the degree of supercooling (Vali 1995).

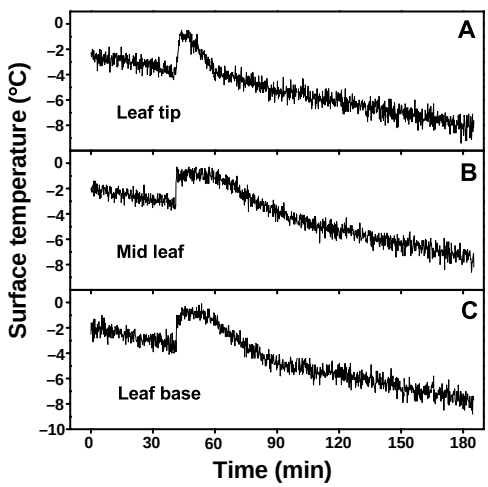

Fig. 6. Time-dependent change in leaf surface temperature during freezing of an intact attached leaf of a snow gum (*Eucalyptus pauciflora*) seedling. Data show exotherms collected from three individual pixels distributed along the midvein of the leaf depicted in Fig. 5. Data were collected at 10-s intervals.

The critical radius for growth of a homogeneously-nucleated ice embryo in aqueous solution supercooled by 3 K is of the order of 20 nm (Wolfe and Bryant 1999). This is somewhat larger than the smaller dimensions of typical aqueous spaces in cell walls so, while cell walls are laden with water (Canny 1995), they resist penetration by growing ice crystals (Wolfe and Bryant 1999). In contrast, the diameters of even the smallest xylem vessels are large relative to the critical radius, so ice can grow along such vessels easily. It is difficult to be specific about the nature of nucleation in xylem vessels. Association of an ice embryo with a vessel wall would reduce the critical free-energy change for crystal growth below that required for homogeneous nucleation. The reduction is a function of the contact angle between the surface and the ice–water interface — the smaller the contact angle, the lower the energy barrier to nucleation (Vali 1995), with the limiting case for homogeneous nucleation being a contact angle of 180°. Contact angles between liquid water and xylem vessels have been found to range from 42–55° in a variety of species (Zwieniecki and Holbrook 2000). If similar contact angles occurred in this instance, the presence of the wall would increase the statistical probability of heterogeneous relative to homogeneous nucleation.

Once nucleation occurred near the leaf petiole, ice grew rapidly through the apoplast, consistent with previous reports (Chen *et al.* 1995). Apparently, the pore sizes in pit membranes of xylem vessels offer little impediment to growth of ice crystals. Ice spread rapidly through the lamina, with crystals developing on mesophyll cell walls. Cell walls collapsed with the dehydrating cells, consistent with observations in wheat (Pearce 1988), rye (Allan *et al.* 1990) and spinach (Hincha and Schmitt 1992). An average T_f of –0.5°C implies a water potential in leaf cells of approximately –0.6 MPa. With a decrease in leaf temperature to –2°C, the water potential of extracellular ice would decline to –2.4 MPa, requiring cell volume to decline by a factor of four to maintain equilibrium, consistent with observations (Fig. 4). Measurements of electrolyte leakage, as a function of nadir temperature during freezing (Fig. 10), showed little leakage at –2°C. However, further cooling to lower temperatures led to a rapid increase in electrolyte leakage (Fig. 10), which in other studies has been shown to result from dehydration-induced destabilization of plasma membranes (Steponkus *et al.* 1993). Thus, small differences in nadir temperatures during freezing would cause large differences in freeze-induced damage to unacclimated tissues.

The present study shows that temperature differences of as much as 4°C develop over a leaf during freezing (Fig. 5) because of spatial variation in both the duration of elevated temperatures (Fig. 9*A*) and the subsequent rates of cooling

(Fig. 9*B*). These differences are related to local variation in water content and thickness of leaves. During freezing, regions where the majority of leaf water freezes quickly will cool more rapidly to lower nadir temperatures than those where prolonged freezing maintains temperatures above ambient. Thus, thinner regions of the leaf near the tip and along the margins are more vulnerable to freezing damage, at least during the time when freezing causes leaf temperatures to be differentially displaced from T_e.

In autumn, for example, considerable freezing damage can occur to unacclimated leaves subject to light frosts. Under such conditions, freezing temperatures sufficient to induce nucleation may not occur until near dawn, and hence may be of short duration. On clear nights with very low wind speed, temperatures of naturally-oriented eucalypt leaves are typically 2°C below ambient air temperature in the absence of frost or dew formation (Leuning 1988; Leuning and Cremer 1988; Ball *et al.* 1997). Thus, given a T_n of –3°C, nucleation could occur in leaves when air temperature was only –1°C. With subsequent increase in leaf temperature to a T_f of, say, –0.5°C, the temperature differential driving heat exchange between a freezing leaf and surrounding air would be much less than in our experimental system, where environmental temperatures continued to decline at 2°C h^{-1}. Thus, the time taken to freeze the majority of leaf water could be much greater than under our experimental

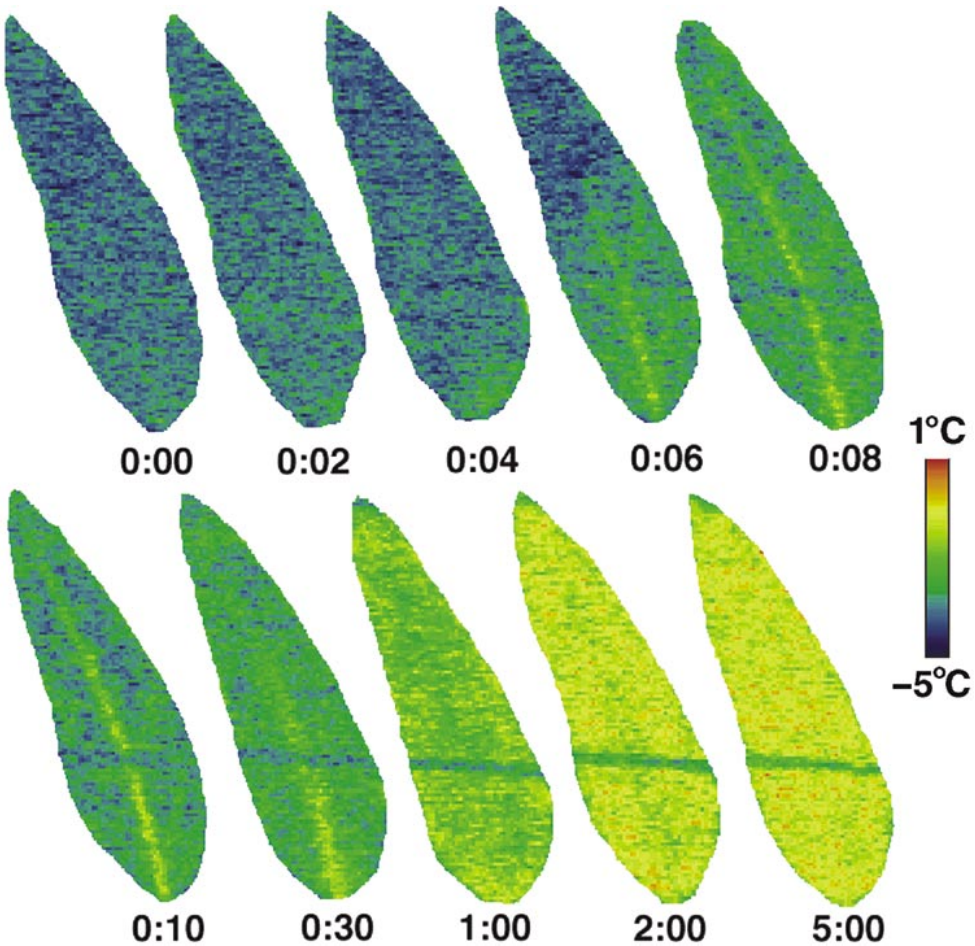

Fig. 7. Spatial variation in leaf surface temperature at selected times during early events in freezing of an intact attached leaf of a snow gum (*Eucalyptus pauciflora*) seedling. Images are arranged in two groups to illustrate spatial changes in leaf temperature associated with two apparent steps in the increase in temperature from T_n to T_f, as shown in exotherms for individual pixels from the same leaf in Fig. 8. The first step was characterized by a rapid increase in temperature following nucleation. There was no detectable ice formation at time 0:00. Two seconds later, nucleation had occurred, raising leaf temperature near the petiole. The ice-front then propagated through the leaf within 8 s, causing a rapid rise in leaf temperature, with temperature increasing more in the midvein than in other regions of the leaf. The second step was characterized by a cooling of leaf temperatures, followed by a slower increase in leaf temperature to T_f, which was similar over the whole leaf. The line across leaf surfaces is due to a rod holding thermocouples in the air space between the leaf and camera.

conditions. These experimental conditions, however, provide a reasonable estimate of freezing times for a high rate of environmental cooling. Even at these high freezing rates, it is clear that the time required to freeze the majority of leaf water is sufficiently long to influence the distribution of freezing damage in unacclimated leaves. Consider, for example, the average data shown in Fig. 9*A*. Twenty minutes after nucleation, leaf temperatures in thin regions of the lamina had returned to the nucleation temperature of –3.1°C, whereas temperatures in thicker regions with a higher water content were still at –0.5°C. If sunrise were to occur at this point, when freezing of the leaf was incomplete, then leaf tissues subject to extracellular freezing at –3.1°C would be much more dehydrated than those where the freezing temperature was closer to T_f. It is apparent from Fig. 10, that such small-scale differences in nadir freezing temperatures would produce major differences in freezing damage, and could account for the characteristic pattern of freeze-induced damage seen during early autumn (Fig. 1).

Previous studies have shown that heat stored in large masses of water can reduce the incidence of lethal freezing temperatures. For example, the high heat capacity of bulky succulents such as cacti buffers sensitive apical tissues from cooling to deleterious temperatures during cold desert nights (Nobel 1980). Similarly, in an African alpine species, exposure of sensitive apical tissues to freezing temperatures is reduced by surrounding stems with large pitcher-like structures filled with water — heat released during prolonged freezing of this external water supply warms the

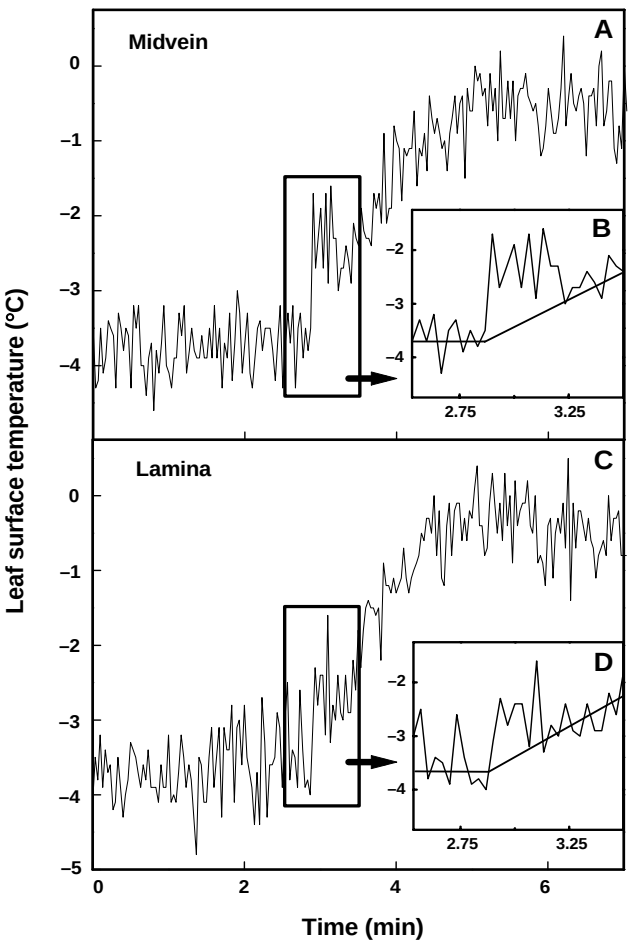

Fig. 8. Time-dependent change in leaf surface temperature during early events in freezing of an intact attached leaf of a snow gum (*Eucalyptus pauciflora*) seedling. Data were collected at 2-s intervals from one pixel in the centre of the midvein (*A*, *B*) and from another pixel in the lamina (*C*, *D*), midway between the midvein and leaf margin of the same leaf shown in Fig. 7. Note that environmental temperature was constant during measurements. Insets highlight small changes in temperature following nucleation.

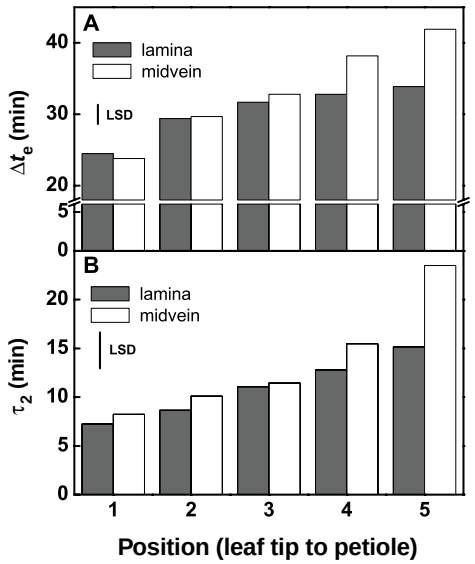

Fig. 9. Spatial variation in (*A*) Δt_e, the time during freezing when leaf surface temperature was elevated above nucleation temperature, and (*B*) τ_2, the characteristic time of cooling once most leaf water had been frozen (see Appendix 1). Values are means for $n = 5$ leaves. Vertical bar denotes the least significant ($P<0.01$) difference between means.

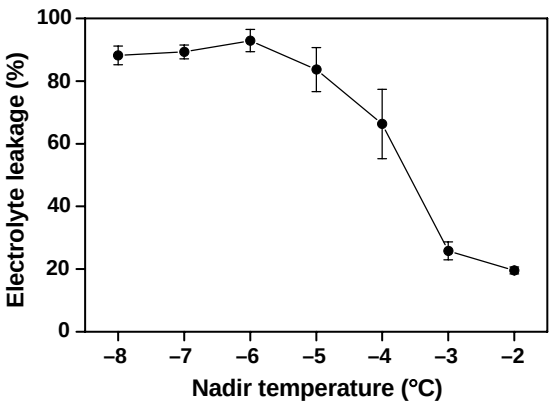

Fig. 10. Electrolyte leakage as a function of nadir temperature in discs from unacclimated leaves of field-grown snow gum (*Eucalyptus pauciflora*) seedlings. Values are means ± s.e., $n = 5$ leaves.

stems, protecting them from excessive nocturnal cooling (Krog *et al.* 1979). Our results, however, show that small differences in water content and thickness also influence minimum leaf temperatures. This would be most important during times of the year when unacclimated leaves are vulnerable to damage from temperatures only slightly below zero. This may contribute to an explanation of the general observation that leaf water content and thickness increase with altitude (Woodward 1979; Körner *et al.* 1983, 1986; Atkin *et al.* 1996). These differences persist if plants originating from high- and low-altitude populations are grown in a common garden (Woodward 1979; Atkin *et al.* 1996), indicating selective pressure to increase leaf thickness and water content. Although increasing leaf thickness would occur at the expense of growth (Atkin *et al.* 1996), one benefit may be reduction in the incidence and severity of freezing injury, particularly when plants are not well acclimated to freezing temperatures. Factors mitigating frost damage may have high selective value, as even damaging but non-lethal frosts can reduce fitness in alpine species, with effects manifest in their population dynamics long after freezing events (Inouye 2000).

Conclusion

The dependence of leaf temperature (T) on position (x, y) is due to the large-scale geometry of the leaf and its surroundings, to availability of water that can freeze, to physical, anatomical and physiological inhomogeneities on anatomical and cellular scales, to the aleatory nature of ice nucleation, and to the thermal history of different regions. A quantitative explanation requires a detailed analysis of the heat balance of local elements of the leaf and their heat exchange with their neighbours, as well as with the environment. We have begun such a study (Frith *et al.* 1999) and shall report it in more detail elsewhere. Here, we have explored some features of the model and found that small-scale inhomogeneities in water content, especially the positions of veins of all sizes and the variation in thickness of leaf tissue, are important to the detailed understanding of spatial variation in leaf T, and hence also freezing damage.

Acknowledgments

Thanks to Dr Cheng Huang and Lewis Ling of Carleton University Facility for Electron Microscopy for assistance with cryo-SEM, Jeff Wilson, Catherine Eadie and Dr Eldon Ball for assistance with photography and preparation of plates, Jack Egerton and Wayne Pippen for expert technical assistance, and Tim Hobbs for permission to grow plants on his farm.

References

Allan WTG, Read ND, Jeffree CE, Steponkus PL (1990) Cryo-scanning electron microscopy of ice formation in rye leaves. *Cryobiology* **27**, 664.

Atkin OK, Botman B, Lambers H (1996) The causes of inherently slow growth in alpine plants: an analysis based on the underlying carbon economies of alpine and lowland *Poa* species. *Functional Ecology* **10**, 698–707.

Ball MC, Egerton JJG, Leuning R, Cunningham RB, Dunne P (1997) Microclimate above grass adversely affects spring growth of seedling snow gum (*Eucalyptus pauciflora*). *Plant*, *Cell and Environment* **20**, 155–166.

Blennow K, Lang ARG, Dunne P, Ball MC (1998) Cold-induced photoinhibition and growth of seedling snow gum (*Eucalyptus pauciflora*) under differing temperature and radiation regimes in fragmented forests. *Plant*, *Cell and Environment* **21**, 407–416.

Canny MJ (1995) Apoplastic water and solute movement: new rules for an old space. *Annual Review of Plant Physiology and Plant Molecular Biology* **46**, 215–236.

Carslaw HS, Jaeger JC (1959) 'Conduction of heat in solids (2nd edn).' (Clarendon: Oxford)

Chen THH, Burke MJ, Gusta LV (1995) Freezing tolerance in plants: an overview. In 'Biological ice nucleation and its applications'. (Eds RE Lee Jr, GJ Warren and LV Gusta) pp. 115–135. (American Phytopathological Society: St Paul, MN)

Frith A, Ball M, Hughes D, Wolfe J (1999) Measurements and models of the spatial distribution of freezing in leaves. *Cryobiology* **39**, 292.

Hincha DK, Schmitt JM (1992) Freeze–thaw injury and cryoprotection of thylakoid membranes. In 'Water and life'. (Eds GN Somero, CB Osmond and CL Bolis) pp. 316–337. (Springer-Verlag: Berlin)

Huang CX, Canny MJ, Oates K, McCully ME (1994) Planing frozen hydrated plant specimens for SEM observation and EDX analysis. *Microscopy Research and Technology* **28**, 67–74.

Inouye DW (2000) The ecological and evolutionary significance of frost in the context of climate change. *Ecological Letters* **3**, 457–463.

Jordan DN, Smith WK (1995) Radiation frost and the relationship between sky exposure and leaf size. *Oecologia* **103**, 43–48.

Körner C, Allison A, Hilscher H (1983) Altitudinal variation in leaf diffusive conductance and leaf anatomy in heliophytes of montane New Guinea and their interaction with microclimate. *Flora* **174**, 91–135.

Körner C, Bannister P, Mark AF (1986) Altitudinal variation in stomatal conductance, nitrogen content and leaf anatomy in different plant life forms in New Zealand. *Oecologia* **69**, 577–588.

Krog JO, Zachariassen KE, Larsen B, Smidsrød O (1979) Thermal buffering in Afro-alpine plants due to nucleating agent-induced water freezing. *Nature* **282**, 300–301.

Landsberg J (1990) Dieback of rural eucalypts: the effect of stress on the nutritional quality of foliage. *Australian Journal of Ecology* **15**, 97–107.

Leuning R (1988) Leaf temperatures during radiation frost. II. A steady state theory. *Agricultural and Forest Meteorology* **42**, 135–155.

Leuning R, Cremer KW (1988) Leaf temperatures during radiation frost. I. Observations. *Agricultural and Forest Meteorology* **42**, 121–133.

Lindow SE, Arny DC, Upper CD (1982) Bacterial ice nucleation: a factor in frost injury to plants. *Plant Physiology* **70**, 1084–1089.

Lutze JL, Roden JS, Holly CJ, Wolfe J, Egerton JJG, Ball MC (1998) Elevated atmospheric [CO_2] promotes frost damage in evergreen tree seedlings. *Plant*, *Cell and Environment* **21**, 631–635.

McCully ME, Shane MW, Baker AN, Huang CX, Ling LEC, Canny MJ (2000) The reliability of cryoSEM for the observation and quantification of xylem embolisms and quantitative analysis of xylem sap *in situ*. *Journal of Microscopy* **198**, 24–33.

Nobel PS (1980) Morphology, surface temperatures, and northern limits of columnar cacti in the Sonoran desert. *Ecology* **61**, 1–7.

Pearce RS (1988) Extracellular ice and cell shape in frost-stressed cereal leaves: a low-temperature scanning electron microscopy study. *Planta* **175**, 313–324.

Pearce RS, Fuller MP (2001) Freezing of barley studied by infrared video thermography. *Plant Physiology* **125**, 227–240.

Peñuelas J, Piñol J, Ogaya R, Filella I (1997) Estimation of plant water concentration by the reflectance water index WI (R900/R970). *International Journal of Remote Sensing* **18**, 2869–2875.

Roderick ML, Berry SL, Saunders AR, Noble IR (1999) On the relationship between the composition, morphology and function of leaves. *Functional Ecology* **13**, 696–710.

Sakai A, Larcher W (1987) 'Frost survival of plants.' (Springer-Verlag: Berlin)

Steponkus PL, Uemura M, Webb MS (1993) A contrast of the cryostability of the plasma membrane of winter rye and spring oat: two species that widely differ in their freezing tolerance and plasma membrane lipid composition. In 'Advances in low-temperature biology. Vol. 2'. (Ed. PL Steponkus) pp. 211–312. (JAI Press: London)

Thomashow MF (1998) Role of cold-responsive genes in plant freezing tolerance. *Plant Physiology* **118**, 1–8.

Uemura M, Steponkus PL (1999) Cold acclimation in plants: relationship between the lipid composition and the cryostability of the plasma membrane. *Journal of Plant Research* **112**, 245–254.

Vali G (1995) Principles of ice nucleation. In 'Biological ice nucleation and its applications' (Eds RE Lee Jr, GJ Warren and LV Gusta) pp. 1–28. (American Phytopathological Society: St Paul, MN)

Webb MS, Gilmour SJ, Thomashow MF, Steponkus PL (1996) Effects of COR6.6 and COR15am polypeptides encoded by *COR* (cold-regulated) genes of *Arabidopsis thaliana* on dehydration-induced phase transitions of phospholipid membranes. *Plant Physiology* **111**, 301–312.

Wisniewski M, Fuller MP (1999) Ice nucleation and deep supercooling in plants: new insights using infrared thermography. In 'Cold-adapted organisms: ecology, physiology, enzymology and molecular biology'. (Eds R Margesin and F Schinner) pp. 105–118. (Springer-Verlag: Berlin)

Wisniewski M, Lindow SE, Ashworth EN (1997) Observations of ice nucleation and propagation in plants using infra-red video thermography. *Plant Physiology* **113**, 327–334.

Wolfe J, Bryant G (1992) Physical principles of membrane damage due to dehydration and freezing. In 'Mechanics of swelling: from clays to living cells and tissues. NATO ASI Series H. Vol. 64'. (Ed. TK Karalis) pp. 205–224. (Springer-Verlag: Berlin)

Wolfe J, Bryant G (1999) Freezing, drying and/or vitrification of membrane solute-water systems. *Cryobiology* **39**, 103–129.

Woodward FI (1979) The differential temperature responses of the growth of certain plant species from different altitudes. II. Analyses of the control and morphology of leaf extension and specific leaf area of *Phleum bertolonii* D.C. and *P. alpinum* L. *The New Phytologist* **82**, 397–405.

Xin Z, Browse J (2000) Cold comfort farm: the acclimation of plants to freezing temperatures. *Plant*, *Cell and Environment* **23**, 893–902.

Zwieniecki MA, Holbrook NM (2000) Bordered pit structure and vessel wall surface properties. Implications for embolism repair. *Plant Physiology* **123**, 1015–1020.

Manuscript received 21 February 2002, accepted 24 June 2002

Appendix 1. A simple model for $T(t)$

For regions and times during which an area of the leaf is thermally homogeneous, one may neglect the contribution of lateral conduction of heat. We also neglect transport of heat by gain or loss of water. We use the linearized equation for the rate of heat loss to the environment, and write:

$$P \cong \varepsilon(T - T_e),$$

where T is the temperature, T_e its value at equilibrium, and ε a constant. At any given time, this is the temperature to which the leaf would equilibrate if radiation and air temperatures suddenly ceased changing. This linearization is discussed in Appendix 2. We consider only the case where water content is fixed. The change in temperature, dT, is determined by the heat capacity, C. Except during freezing:

$$dT = -\frac{P}{C}\,dt = -\frac{\varepsilon(T - T_e)}{C}\,dt.$$

In the experiments here, air and radiation temperatures decline linearly, so put $T_e \cong T_o + \alpha t$ where α (< 0) is a constant chosen by the experimentalist. The preceding differential equation has the solution:

$$T = T_o + \alpha(t - \tau) + \Delta T\, e^{-t/\tau},$$

where $\tau = C/\varepsilon$.

ΔT is a parameter that depends upon thermal history. This exponential approach to a linear fall in T is expected before freezing commences. It would also be expected after freezing is completed, but the required conditions for Newtonian cooling, including constant mass and specific heat, may not be fulfilled under the experimental conditions. Detailed discussion of phenomena associated with heat transfer are given by Carslaw and Jaeger (1959).

Appendix 2. Linearization of the heat exchange parameters

Net radiation loss per unit area may be written as:

$$P'_r = g(e_l T^4 - e_b T_b^4),$$

where T is the temperature of the leaf and T_b is that of the radiation background, e_l and e_b are the emissivities, and g is a factor that includes the solid angle available for radiation. This function may be linearized as follows. Define T_r so that:

$$e_l T_r^4 = e_b T_b^4,$$

i.e. T_r is the temperature that the leaf would reach if it equilibrated with the background radiation, in the absence of heat conduction. Let $z = T - T_r$, so:

$$P'_r = g e_l (T_r + z)^4 - e_b T_b^4 = g e_l (T_r^4 + 4 z T_r^3 + 12 z^2 T_r^2 + \text{etc.}) - g e_b T_b^4$$

$$\cong 4 g e_l T_r^3 (T - T_r)$$

$$P'_r = \alpha(T - T_r),$$

where $\alpha = 4 g e_l T_r^3 = 4 g e_b T_b^4$.

The dependence of heat conduction to the air, although a complicated function, may also be linearized:

$$P'_c = \beta(T - T_a),$$

where 'a' refers to the air, and β is a constant. If the leaf temperature finally comes to thermal equilibrium, it has temperature T_e, where:

$$\alpha(T_e - T_b) + \beta(T_e - T_a) = 0, \text{ so:}$$

$$T_e = \frac{\alpha T_b + \beta T_a}{\alpha + \beta}.$$